

Document Version

Final published version

Citation (APA)

Pimenta, M., Gürleyük, Ç., Walsh, P., O’Keeffe, D., Babaie, M., & Makinwa, K. (2020). A 200 μ W Eddy Current Displacement Sensor with 6.7nm_{rms} Resolution. In *2020 IEEE Symposium on VLSI Circuits: Proceedings* (pp. 1-2). Article 9162849 IEEE. <https://doi.org/10.1109/VLSICircuits18222.2020.9162849>

Important note

To cite this publication, please use the final published version (if applicable).
Please check the document version above.

Copyright

In case the licence states “Dutch Copyright Act (Article 25fa)”, this publication was made available Green Open Access via the TU Delft Institutional Repository pursuant to Dutch Copyright Act (Article 25fa, the Taverne amendment). This provision does not affect copyright ownership.
Unless copyright is transferred by contract or statute, it remains with the copyright holder.

Sharing and reuse

Other than for strictly personal use, it is not permitted to download, forward or distribute the text or part of it, without the consent of the author(s) and/or copyright holder(s), unless the work is under an open content license such as Creative Commons.

Takedown policy

Please contact us and provide details if you believe this document breaches copyrights.
We will remove access to the work immediately and investigate your claim.

Green Open Access added to TU Delft Institutional Repository

'You share, we take care!' - Taverne project

<https://www.openaccess.nl/en/you-share-we-take-care>

Otherwise as indicated in the copyright section: the publisher is the copyright holder of this work and the author uses the Dutch legislation to make this work public.

A 200 μ W Eddy Current Displacement Sensor with 6.7nm_{RMS} Resolution

Matheus Pimenta^{1,2}, Çağrı Gürleyük¹, Paul Walsh², Daniel O’Keeffe², Masoud Babaie¹, Kofi Makinwa¹

¹ Delft University of Technology, Delft, The Netherlands, ² Cypress Semiconductor, Cork, Ireland

Abstract

This paper describes a low-power eddy current displacement sensor intended for safety-critical touch applications. A sensing inductor is incorporated into a digital PLL to efficiently digitize the displacement of a flexible metal foil. At a stand-off distance of 500 μ m, the sensor achieves 6.7nm resolution in a 3kHz bandwidth over a 43 μ m range. It consumes 200 μ W from a 1.8V supply, which represents a 35x improvement on the state of the art.

Introduction

Eddy current sensors (ECSs) are often used for high-resolution displacement sensing [1,2]. Compared to capacitive sensors, they are more robust to humidity and dust, while also providing galvanic isolation [3]. This makes them an attractive option in safety-critical touch applications [4]. However, the high power consumption (>10mW) of previous high-resolution designs [1-3] is a major drawback, especially when multiple sensor nodes are required.

As illustrated in Fig. 1a, a galvanically-isolated touch sensor can be realized by placing a flexible metal foil near a sensing coil that forms part of an LC oscillator. The AC currents in the coil will then induce eddy currents in the foil, whose amplitude increases when a touch reduces the foil/coil spacing. This reduces the coil’s inductance and quality factor, and changes the oscillator’s output amplitude and frequency. In [1-3], displacement is determined by sensing oscillation amplitude with a wide-bandwidth front-end, resulting in high power consumption. In this work, the oscillator is embedded in a digital bang-bang PLL, which digitizes the touch-induced changes in coil inductance. This allows the power-hungry front-end to be replaced by a low power comparator-based phase-frequency detector (PFD).

Architecture and Implementation

Fig. 1b shows the block diagram of the touch sensor. The sensing coil L_{sen} and a programmable capacitor DAC form the tank of a digitally-controlled oscillator (DCO) with an average output frequency $f_{DCO} \sim 24$ MHz. The DCO is embedded in a bang-bang PLL, which locks the DCO’s output phase to the rising edges of a reference clock f_{ref} . To save power, the PLL sub-samples the DCO output, such that $f_{ref} = f_{DCO}/8 = 3$ MHz. A low-power comparator-based PFD establishes whether the DCO phase is leading or lagging (Fig. 2a). Its output is filtered by a 1st-order digital loop filter (DLF), 1-bit quantized (BS) and then used to drive a unit DAC element (C_{fin}) such that, on average, $f_{DCO} = 8 * f_{ref}$. At steady-state, the bitstream average will be a digital representation of the change in L_{sen} and, hence, of the displacement X_{act} of the metal foil (Fig. 2b). The use of a DLF allows loop stability to be flexibly tuned to match the requirements of different foil/coil configurations.

As shown in Fig. 3, the DCO is based on a complementary cross-coupled LC oscillator. Since the nominal stand-off distance X_{so} , is application dependent and is much larger than the touch-induced displacement X_{act} , the capacitive DAC is split into a 5-bit coarse DAC (C_{cs}) and a 1-bit fine DAC (C_{fn}). The choice of C_{cs} (24pF in total) allows f_{DCO} to be set to ~ 24 MHz for a range of PCB coil configurations and stand-off distances ($500\mu\text{m} < X_{so} < 1\text{mm}$). The choice of C_{fn} (1.6pF) is

commensurate with the maximum expected X_{act} ($\sim 40\mu\text{m}$). To minimize their “OFF” capacitance, and thus maximize the DCO’s tuning range, large (1.25M Ω) resistors are used to reverse-bias the drain/source-to-bulk diodes of the coarse DAC switches. Instead of the biasing resistors, C_{fn} DAC uses two transistors to minimize its switching time. The transconductance of the cross-coupled pair can be tuned via a tail-current DAC, ensuring robust oscillator start-up for different sensor geometries, and allowing its phase noise to be optimized.

In this system, the main sources of noise are the DCO’s phase noise and the quantization noise originating from the PFD and the 1-bit quantizer at the DLF output. Since both the oscillator and the DLF act as integrators, quantization noise at the DLF output will be 2nd-order shaped, while the PFD’s quantization noise and the DCO’s phase noise will be 1st-order shaped. DCO’s phase noise (due to thermal noise) has a $1/f^2$ characteristic around the carrier frequency. After 1st-order shaping, this dominates the in-band noise of the output bitstream and thus determines the resolution of the system.

Measurement Results

Fabricated in 0.18 μ m CMOS, the ECS occupies 0.21 mm² (Fig. 7a) and consumes 200 μ W from a 1.8V supply. As depicted in Fig. 7b, it was characterized with a copper target mounted on a linear stage and a sensing coil made on a two-layer standard FR4 PCB (5mm diameter, $L_{sen}=500$ nH). The bitstream output was decimated by an external sinc² filter.

Fig. 4 shows the decimated ECS output as a function of displacement. For X_{so} of 500 μ m and 1mm, the full-scale range is 43 μ m (6.7nm_{RMS} resolution) and 135 μ m (26.8nm_{RMS} resolution), respectively. Sensor resolution was obtained from the standard deviation of 3300 consecutive samples (Fig. 4b). Since sensitivity decreases with stand-off distance, the resolution at $X_{so}=1$ mm is lower, but still is about 12b ENOB. Fig. 5 shows the power spectral density of the ECS output bitstream at $X_{so}=500\mu\text{m}$. The ECS achieves an SNR of 76.4dB in a 3kHz bandwidth, corresponding to an equivalent displacement noise of 6.7nm_{rms}. Out-of-band noise is initially dominated by reference phase noise and the PFD’s quantization noise (20dB/dec) and then by the quantization noise at the DLF output (40dB/dec). Fig. 6 shows the sensor response to a touch event at $X_{so}=1$ mm, where a 2 μ m displacement of the metal target can be reliably observed.

A comparison with the state-of-the-art is shown in Table I. Compared to [1-5], this work achieves the highest FoM, and the smallest die area, while consuming 35x less power. This enables the ECS to be used in safety-critical, multi-node touch applications. Moreover, the digital-intensive design benefits from technology scaling, promising to achieve even better energy and area efficiency.

References

- [1] V. Chatuverdi et al., *ISSCC*, 2017.
- [2] V. Chatuverdi et al., *VLSI*, 2017.
- [3] A. Fekri et al., *ESSCIRC*, 2014.
- [4] LDC2112, <https://www.ti.com/product/LDC2112>
- [5] M. Oberle, et al., *JSSC*, 2002.

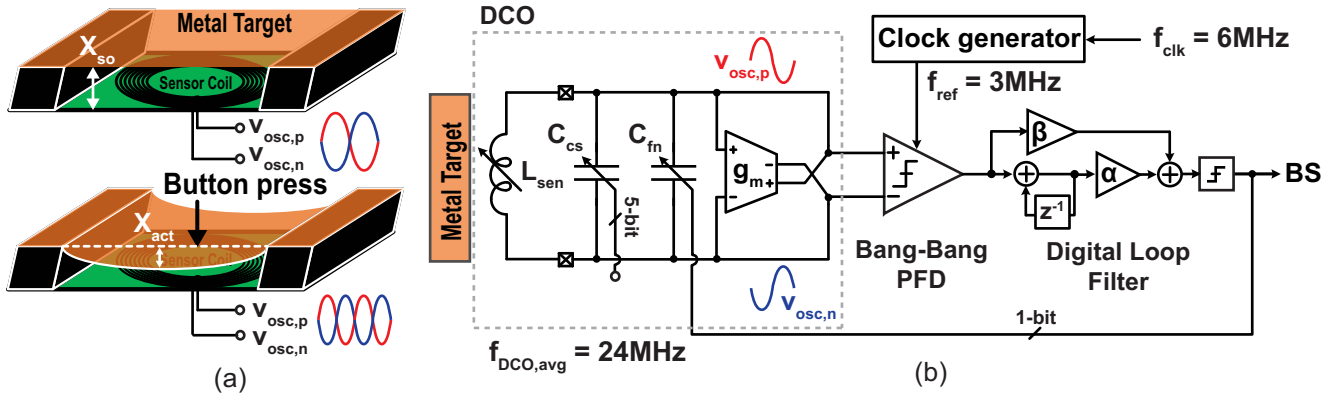


Fig. 1 ECS touch sensor application (a) and system block diagram (b)

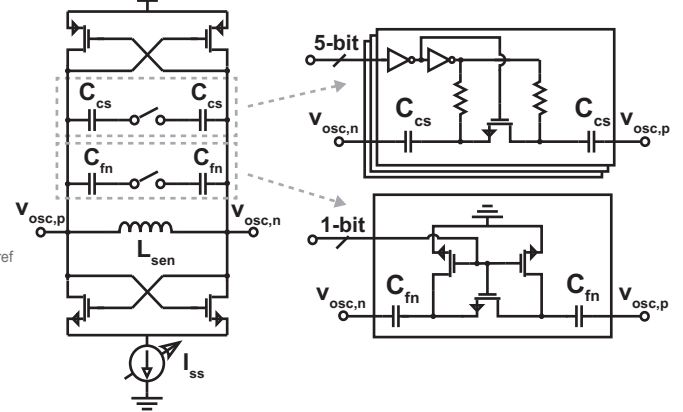
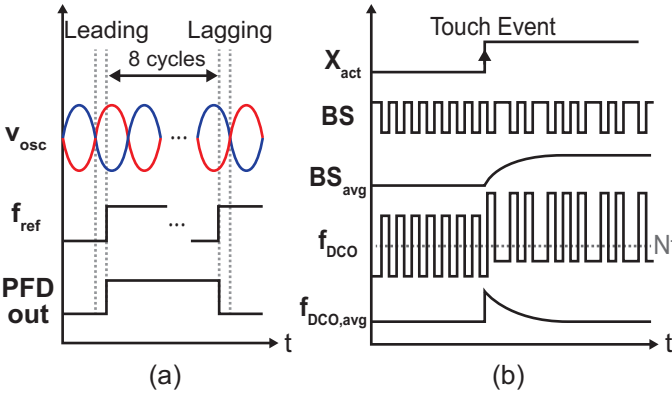


Fig. 2 Timing diagram of the comparator based phase-frequency detector (a) and system response to a touch event (b)

Fig. 3 Schematic of the digitally controlled oscillator (DCO)

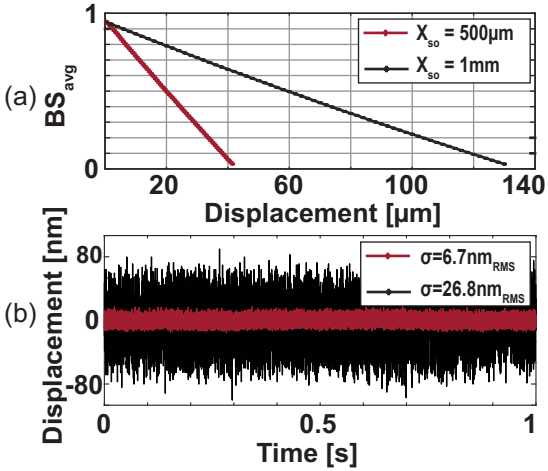


Fig. 4 Bitstream vs. displacement (a) and displacement noise at steady-state (3300 samples) (b)

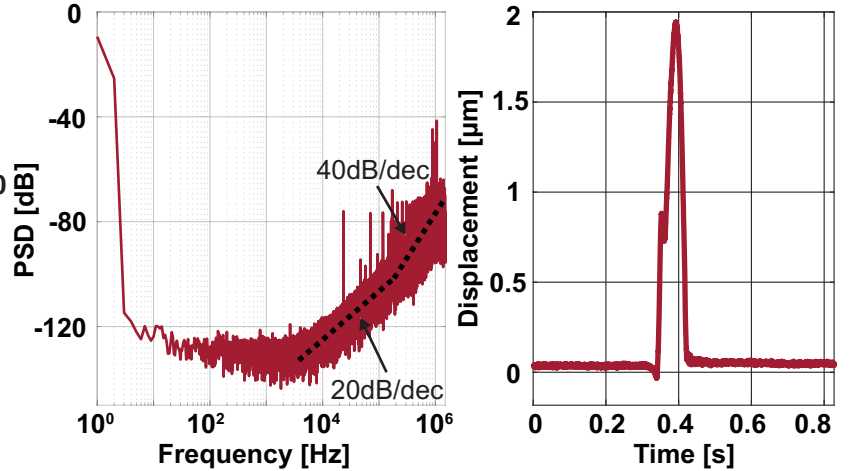


Fig. 5 Output power spectral density (PSD) vs. Frequency [Hz] and Displacement [μm] vs. Time [s]

Table I. Performance summary and comparison

	This Work	[1]	[2]	[3]	[4]	[5]
Tech. [μm]	0.18	0.18	0.18	0.35	-	0.6
Area [mm^2]	0.207	1.177	0.264	3.94	-	13
X_{so} [m]	500 μ	105 μ	55 μ	3m	500 μ	3m
f_{sen} [MHz]	24	126	145	15	24	0.312
ENOB	12.7	14.1 [#]	12.4	15	12	10
Res. [nm]	6.7	0.6	1.85	135	~100 ^{&}	2930
BW [kHz]	3	2	2	1	1	10
Power [mW]	0.200	19.8	9.1	18	3.4 ^{&}	7.3
FoM [nm^2J]*	3.0 μ	3.6 μ	15 μ	328m	34m	6.27

* Resolution FoM = resolution² × power/BW [#] Analog output

[&] Considering a similar L_{sen} , X_{so} and f_{sen}

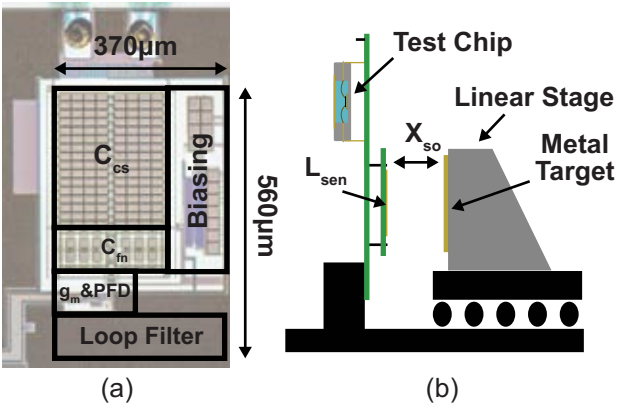


Fig. 7 Die micrograph (a) and test setup (b)